Since January 2020 Elsevier has created a COVID-19 resource centre with free information in English and Mandarin on the novel coronavirus COVID-19. The COVID-19 resource centre is hosted on Elsevier Connect, the company's public news and information website.

Journal of Chromatography B 1206 (2022) 123363

Contents lists available at ScienceDirect

Journal of Chromatography B

journal homepage: www.elsevier.com/locate/jchromb

A validated LC-MS/MS method for determination of antiviral prodrug molnupiravir in human plasma and its application for a pharmacokinetic modeling study in healthy Egyptian volunteers

Amira S. Gouda [a], Hoda M. Marzouk [b,*], Mamdouh R. Rezk [b], Ahmed M. Salem [c,d], Mosaad I. Morsi [a], Eman G. Nouman [a], Youmna M. Abdallah [a], Ahmed Y. Hassan [a], Ahmed M. Abdel-Megied [e,f]

[a] Zi-diligence Biocenter, Bioequivalence Research, El-Mokattam, Cairo, Egypt
[b] Analytical Chemistry Department, Faculty of Pharmacy, Cairo University, Kasr El-Aini Street, 11562 Cairo, Egypt
[c] Department of Pharmaceutical Sciences, University of Maryland School of Pharmacy, Baltimore MD 21201, USA
[d] Clinical Pharmacy Department, Faculty of Pharmacy, Ain-Shams University, Cairo, Egypt
[e] Pharmaceutical Analytical Chemistry Department, Faculty of Pharmacy, Kafr El-Sheikh University, Kafr El-Sheikh City, Egypt
[f] Department of Pharmaceutical Sciences, Notre Dame of Maryland School of Pharmacy, Baltimore, MD 21210, USA

ARTICLE INFO

Keywords:
SARS-CoV-2
Molnupiravir
LC-MS/MS
Population Pharmacokinetic Modeling
NHC

ABSTRACT

A fully validated, simple, rapid and reproducible liquid chromatography-tandem mass spectrometry method was developed to determine NHC (N-hydroxycytidine), the active metabolite of Molnupiravir (MOL) in human plasma; one of the limited treatment options for SARS-CoV-2 in plasma of healthy volunteers. The internal standard (IS) used was ribavirin. The extraction of analyte and IS from plasma was performed using acetonitrile as a solvent for protein precipitation. Agilent Zorbax Eclipse plus C_{18}, 4.6 × 150 mm, (5 μm) was used for chromatographic separation using a mixture of methanol0.2 % acetic acid (5:95, v/v) as a mobile phase that was pumped at a flow rate of 0.9 mL/min. Detection was performed on a triple quadrupole mass spectrometer operating in multiple reaction monitoring (MRM) employing positive ESI interface using API4500 triple quadrupole tandem mass spectrometer system, with the transitions set at *m/z* 260.10 → 128.10 and 245.10 → 113.20 for NHC and IS respectively. Method validation was performed in accordance with United States FDA bioanalytical guidance. The concentration range of 20.0–10000.0 ng/mL was used to establish linearity via weighted linear regression approach ($1/x^2$). Moreover, the analyzed pharmacokinetic data from twelve Egyptian healthy volunteers were used to develop a population pharmacokinetic model for NHC. The developed model was used to perform simulations and evaluate the current MOL dosing recommendations through calculating the maximum concentration (C_{max}) "the safety metric" and area under the curve ($AUC_{0\text{-}12\ h}$) "the efficacy metric" for 1000 virtual subjects. Geometric mean ratios (GMR) with their associated 90% confidence intervals (CI) compared to literature values were computed. Geometric means of simulation-based Cmax and AUC0-12 were 3827 ng/mL (GMR = 1.05; 90% CI = 0.96–1.15) and 9320 ng.h/mL (GMR = 1.04; 90% CI = 0.97–1.11), respectively indicating that current MOL dosage can achieve the therapeutic targets and dose adjustment may not be required for the Egyptian population. The developed model could be used in the future to refine MOL dosage once further therapeutic targets are identified.

1. Introduction

COVID-19; a disease that was first reported in China and has taken a lot of lives since 2020. The urge for the finding of therapy is crucial to eradicate COVID-19. Hence, a lot of strategies are being followed to discover an improved treatments for COVID-19 [1–3]. Early treatment of patients with confirmed COVID-19 who demonstrate mild symptoms only is one of those strategies, aiming to decrease the number of patients that develop to more severe disease and necessitate hospitalization or admittance to intensive care unit (ICU) [4]. Amongst those treatments is

* Corresponding author at: Lecturer of Analytical Chemistry, Faculty of Pharmacy, Cairo University, Egypt.
E-mail address: hodaallah.marzouk@pharma.cu.edu.eg (H.M. Marzouk).

https://doi.org/10.1016/j.jchromb.2022.123363
Received 27 May 2022; Received in revised form 1 July 2022; Accepted 3 July 2022
Available online 5 July 2022

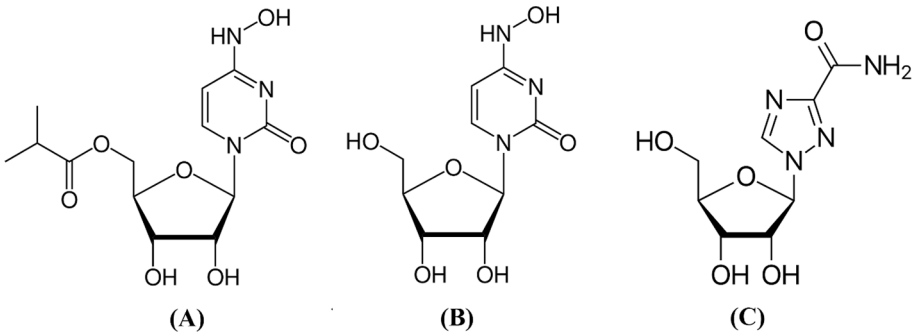

Fig. 1. Chemical structure of Molnupiravir (MOL) (A), Molnupiravir active metabolite, NHC (B) and the internal standard, Ribavirin (C).

Molnupiravir (MOL), which has recently gained emergency use authorization by the United States Food and Drug Administration (US-FDA) for treatment of mild-to-moderate SARS-CoV-2 cases. MOL is a pyrimidine ribonucleoside analogue (also known as EIDD-2801/MK-4482) with a chemical name of ((2R,3S,4R,5R)-3,4-dihydroxy-5-(4-(hydroxyamino)-2-oxopyrimidin-1(2H)-yl) tetrahydrofuran-2-yl) methyl isobutyrate, Fig. 1**A**. MOL is a prodrug which is quickly metabolized to the ribonucleoside analogue N-hydroxycytidine (NHC) also known as EIDD-1931, Fig. 1**B.** NHC appears quickly in plasma and gives the maximum concentration in serum with a median time of 1.00 to 1.75 h. Then, its concentration in serum declines gradually with a half-life of nearly 1 h [5]. NHC is not protein-bound and has an estimated volume of distribution (V_d) of 142 L. Elimination of NHC follows linear pharmacokinetics (PK) through the same pathways of eliminating the endogenous pyrimidines where NHC is metabolized to uridine and cytidine with an estimated clearance (CL) of 76.9 L/hour. Liver and kidney play minor role in eliminating NHC, hence, dose modification is not required for hepatic or renal impairment [6].

Once NHC enters cells, it undergoes phosphorylation to form the active moiety, ribonucleoside triphosphate (NHC-TP). Viral RNA polymerase incorporates NHC-TP into the viral RNA, leading to accumulation of errors in the viral genome and inhibition of replication [4]. Preliminary clinical-trial results showed that MOL can significantly reduce hospitalizations and deaths from COVID-19 by approximately 50% [7].

To the best of authors' knowledge, only one published study in healthy volunteers was found describing the PK for MOL active metabolite NHC [5], where the study was performed on capsules and oral solution formulations but no reported data for tablet's PK parameters. Moreover, a data from only 6 healthy volunteers was presented in this study without full description of the bioanalytical method used, while in our proposed work data from 12 healthy volunteers were presented using a completely validated LC-MS/MS bioanalytical method and a detection limit that was sufficient to detect all volunteers' sampling intervals. Another two LC-MS/MS methods were reported for MOL, one used spiked human plasma [8] and the other used human plasma and saliva [9] but both didn't represent the pharmacokientic parameters for MOL active metabolite; NHC unlike the presented work which fully describes the PK for NHC in healthy Egyptian volunteers. Moreover, the analyzed PK data were used to develop a population PK model for NHC which could be used in the future to refine MOL's dosage once further therapeutic targets are identified.

Consequently, the primary goal of the presented study was to accurately present the PK parameters for the novel antiviral MOL through a well established and fully validated LC-MS/MS method in agreement with the US-FDA guidelines for bioanalytical method validation [10], where LC-MS/MS methods are exceedingly sensitive and specific analytical techniques that can precisely determine the identities and concentration of compounds either as parent drugs [2,3,11–14] or metabolites in biological matrices[15]. The second goal was to construct a population PK model for NHC and evaluate through simulations the current MOL dosing recommendations of 800 mg every twelve hours for five days in achieving the therapeutic targets in the Egyptian population.

2. Materials and methods

2.1. Chemicals and reagents

NHC (98.4%, as per the provider COA) was obtained from Zhejiang Hongyuan Pharmaceutical Co., Ltd (Zhejiang, China). Ribavirin (IS) was obtained from Hubei Yitai Pharmaceutical Co., Ltd, (Hubei,China) with a purity of 99.7%. Ultra-pure water, acetic acid, methanol, and Acetonitrile (HPLC grade) were provided from Merck (Gernsheim, Germany). Blank human plasma was provided from VACSERA, Giza, Egypt; Batch No. 20080249, 20070228, 20050315, 20050302, 20000469, 20001244, Haemolyzed plasma; 1,705,241 and Lipemic plasma; 171128001.

2.2. Pharmaceutical formulations

Molnupiravir 800 mg Tablets, containing 800 mg MOL per tablet, produced by Eva Pharma, Egypt, Batch No.: 2107414.

2.3. Instrumentation

A triple quadrupole tandem mass spectrometer API4500 coupled with Exion HPLC system (ABSciex, Canada) was operated for the quantitative analysis of NHC. Control of hardware and processing of data were performed utilizing Analyst 1.6.3 software (ABSciex, Canada).

2.4. Liquid chromatographic and mass spectrometric conditions

Agilent Zorbax Eclipse plus C_{18}, 4.6 × 150 mm, (5 μm); (Agilent, USA) was used for chromatographic separation. Column oven temperature was kept at 40 °C, a 5 μL of samples were injected to liquid chromatograph using isocratic elution system comprised of 0.2% acetic acid–methanol (5:95, v/v) at a flow rate of 0.9 mL/min. the total run time was 3.0 min. Ultrasonication to mobile phase parts was performed before usage for 10 min. By adjusting the MRM mode with a positive ESI interface, ions of NHC were detected at the following transitions: *m/z* 260.10 → 128.10 and 245.10 → 113.20 for the IS, the nitrogen was used as the auxiliary curtain and collision gas, while the nebulizer gas was air (zero grade). The LC-MS/MS source parameters were set in the following manner: the curtain and collision gas were 30 and 10 psi in order; while source temperature was 450°C; the ion source gas (GS1) was 45 psi while the drying gas (GS2) was 40 psi; the ion spray voltage was set as 4000 V and 4000 V for NHC and IS, in order.

2.5. Standard solutions, calibrators and quality control samples

Stock solutions for NHC and IS were performed in 100-mL volumetric flask containing acetonitrile to obtain 200 μg/mL and 100 μg/mL respectively. Serial working standard solutions of NHC were further

performed via dilution in the same solvent. Calibration curves were prepared by spiking 50 μL from each NHC working solution and 50 μL of IS into 450 μL blank plasma. The calibration standards were performed to cover a concentration range of (20.0 – 10000.0 ng/mL). Quality Control sets were arranged at 20.0 ng/mL (lower limit of quantification quality control, LLOQ), 60.0 ng/mL (low quality control, Low QA), 800.0 ng/mL (middle quality control, Mid QC-A), 3000.0 ng/mL (middle quality control, Mid QC-B) and 8000.0 ng/mL (high quality control, High QC), as demonstrated in **Table S1**.

2.6. Sample preparation

Prior to analysis, thawing of frozen plasma samples was carried out at room temperature. The plasma samples were spiked with the drug and internal standard, then precipitation of plasma proteins was accomplished by the addition of one and half milliliters of acetonitrile, samples were then mixed using vortex mixer for 4 min, the centrifugation was carried out at 2795 xg at 4 °C for another 5 min. The upper apparent solution was evaporated using vacuum concentrator at 45 °C, then reconstitution with 500 μL of water was performed, finally an aliquot of 5 μL was injected into the LC-MS/MS system.

2.7. Bioanalytical method validation

United States FDA guideline for bioanalytical method validation [10] was used as a guide in method validation for the bioanalysis of NHC, and then application to PK study of MOL tablets.

2.7.1. Selectivity

Suggested method selectivity was evaluated using 6 batches from different sources of blank human plasma along with lipemic and hemolyzed plasma samples to demonstrate the lack of interference from the internal plasma components and concomitantly used medications in the chromatographic system.

2.7.2. Linearity and range

The plasma calibration curves were obtained by plotting peak area ratio of NHC to that of ribavirin (IS) against the corresponding concentrations. Concentrations for NHC were 20.0, 100.0, 500.0, 1000.0, 2000.0, 6000.0, 9000.0, 10000.0 ng/mL and weighted ($1/x^2$) regression was used. The deviation at lowest calibration point (LLOQ) should be ± 20% of the nominal values, while other sets variation is allowed to be ± 15%.

2.7.3. Carry-over

Carry-over of NHC and IS was evaluated after injection of blank samples after the highest calibration standard (ULOQ), to confirm that no potential carry-over of NHC and IS could affect the accuracy and precision of the method. The blank sample's carry over should not be more than 20% of NHC response at the LLOQ and 5% of the response for IS.

2.7.4. Precision and accuracy

This was assessed by analyzing the quality control (QC) samples at concentrations of LLOQ, Low, Mid and High QC. The intra-day and inter-day precision of the procedure were evaluated after injecting six replicates (n = 6) in the same day and over three different days for each concentration level which demonstrated as (coefficient of variation, RSD %). Proposed method accuracy was demonstrated as % bias which should be within 15% for the QC samples, however a variation of ± 20% of the nominal values was accepted for LLOQ.

2.7.5. Extraction recovery and matrix effect

This was done by comparing the peak responses of NHC extracted at four levels (20.0, 60.0, 800.0, 3000.0 and 8000.0 ng/mL) to those of blanks spiked with the un-extracted analytes at the same concentrations. The Recoveries of both NHC and IS (at least) 50% are required. Assessing matrix effect was executed using six different blank plasma samples along with lipemic and hemolyzed plasma samples. The Matrix Factor (MF) was investigated via comparing the ratio of the peak area of the blank samples where the matrix was spiked with the analytes after the extraction to those prepared in standard solution (in absence of matrix) at the same concentration.

2.7.6. Dilution integrity

Spiking the matrix with concentration of the analytes above the ULOQ was done to investigate the dilution integrity using six replicates (n = 6) then dilution using blank matrix is performed. The variation in Accuracy and precision should be within ± 15%.

2.7.7. Stability

The stability of NHC in human plasma was evaluated by analyzing six samples of low and high QC (n = 6) compared to freshly prepared QCs. The bench-top stability of NHC in plasma was measured for the defrosted samples at room temperature then left for 18 h before analysis, also it was assessed in human whole blood after comparing the samples kept at room temperature for 6 h with freshly prepared ones. The processed sample stability was investigated by maintaining the QCs samples in auto-sampler at 15 °C for 20 h followed by analysis. Samples were stored at −70 ± 15 °C for a period of 16 days to evaluate long-term stability. The freeze (-70 ± 15 °C) and thaw (room temperature) stability were conducted under the conditions of 5 freeze and thaw cycles. All samples are considered stable with RSD ± 15%.

2.7.8. Incurred plasma samples reanalysis

Incurred samples were re-analyzed to demonstrate the perceived robustness of the proposed bioanalytical method. Evaluation of ISR data was performed after calculating the mean of two concentrations and then based on the differences between original and repeat value from this mean concentration where at least two-thirds of the repeats agree within 20 % of the mean concentration for chromatographic assays.

2.8. Subjects and data

Twelve subjects were screened, enrolled and completed this study. Inclusion criteria included age (18–50 years), body mass index (18.5–30.0 kg/m^2) and normal observations for physical examination along with normal electrocardiogram, body temperature, pulse rate, respiratory rate and blood pressure, negative drug abuse test, negative alcohol in urine and normal laboratory examinations. Exclusion criteria comprised history of allergy to MOL, alcoholism, or presence of significant medical disease; diabetes or any disease which could compromise the haemopoietic, gastrointestinal, renal, hepatic, cardiovascular, and respiratory or central nervous systems.

The subjects were informed about the objectives of the study then requested to sign the ICF. The research protocol was accepted by the relevant IEC of Zi-Diligence biocenter, Egypt number 09/2021, dated on October 13, 2021. In addition, all study procedures were based on the international conference on harmonization, E6 Good Clinical Practice (ICH, E6GCP) guidelines.

Twelve subjects received a single oral dose of MOL 800 mg tablets after overnight fasting for 10 h but drinking water was freely available. Oral administration of the drug was performed in randomized way using a 240 mL water. Fasting is required for another four hours and half and water was not allowed for drinking from 1 h before dosing till 2 h after dosing. Collection of blood samples was done using heparin vacutainers at zero time and 0.25, 0.50, 1.00, 1.50, 2.00, 2.50, 3.00, 4.00, 6.00, 9.00 and 12.00 h post-dose as per the research protocol. Plasma samples were obtained by centrifugation at 1006 xg for 10 min and stored at −70 ± 15 °C for until analyzed.

In addition to the received dose and measured concentrations, the data contained the following demographic and laboratory data for each

patient: age, height, weight, body mass index, smoking status, race, sex, blood sugar level, blood urea, creatinine, aspartate aminotransferase, alanine amino transferase, alkaline phosphatase, sodium, potassium, total bilirubin, total cholesterol, high density lipoprotein, low density lipoprotein, triglycerides, and total proteins.

2.9. Population PK modeling of NHC, the active form of MOL

2.9.1. Base model building

Different absorption and disposition structural PK models were explored to fit NHC concentration time profiles as described previously [16]. Log-normal distribution was used to describe inter-individual variabilities (IIV) on PK parameters and multiple residual error models such as additive, proportional and combined error models were tried to describe the data [17].

Choosing between candidate models included multiple aspects and statistical criteria such as: change in objective function value $\geq$ 3.84 units assuming chi-square distribution with significance level of 0.05 and one degree of freedom. Other statistical criteria included: Akaike information criterion (AIC) and Bayes information criterion (BIC). In addition, goodness-of-fit plots and precision of PK parameter estimates were evaluated.

Given that considerable NHC concentrations were below the lower limit of quantification, the M3 method was used to fit NHC PK data where all values below the lower limit of quantification were considered as censored observations, as described previously by Beal [18].

Non-linear mixed effect modeling and estimation of population PK parameters were conducted in MonolixSuite version 2020R1 (Lixoft®) using the Stochastic Approximation Expectation Maximization (SAEM) algorithm. Data processing and manipulations were done in R-Studio statistical software (R Foundation for Statistical Computing, Vienna, Austria).

2.9.2. Covariate model building

Candidate covariates such as: body weight, total protein, serum creatinine, liver function and age were assessed for association with specific PK parameters according to following criteria: i) biological plausibility according to knowledge about PK of the drug, ii) exploratory analysis of the correlation between individual random effects and covariates, iii) reduction in IIV of PK parameter following the covariate incorporation as well as evaluation of statistical criteria as described previously. Body weight was assessed as potential covariate for both apparent clearance (CL/F) and volume of distribution (V_d/F) according to allometric scaling principles [19].

2.9.3. Model evaluation

Standard diagnostic plots such as: observations versus population predictions, observations versus individual predictions, Individual weighted residuals (IWRES) versus time after the dose and IWRES versus population predictions were assessed for any model misspecifications. Median PK parameter values with associated 95% confidence intervals (CI) obtained from nonparametric bootstrapping (n = 500 replicates) were calculated and compared to those generated during model fitting process to assess the robustness of the final PK parameter estimates. Finally, prediction corrected visual predictive check (pcVPC) was generated based on 500 simulations to examine the agreement between NHC observed concentrations and final PK model-based simulated concentrations.

2.9.4. Simulations to evaluate the current dosing recommendations for MOL in egyptians

Final population PK parameters were used to simulate NHC concentration time profiles for 1000 virtual subjects following the administration of currently approved 800 mg oral dose of MOL twice daily for 5 days[20]. The distribution of body weight in the virtual population was proposed to follow log-normal distribution having mean of 81.5 kg and coefficient of variation of 25% to match the body weight distribution in the previously published cohort [4]. Female-to-male ratio was set to 1:1 ratio [20] and effect of sex covariate on V_d/F of NHC was simulated according to a previously published covariate model as following [4]:

$$Vd/F_i = tvVd/F \cdot (1 - 0.33 \cdot SEX_i)$$

Where Vd/F_i is the volume of distribution of the *ith* virtual subjects, tvVd/F is the typical PK estimate of NHC's volume of distribution and SEX_i is the sex of the *ith* virtual subject where zero indicates male and one indicates female.

Model-based C_{max} "PK metric for safety" and $AUC_{0\text{-}12}$ "the PK metric for efficacy" were computed. Geometric mean ratios (GMR) and the associated 90% confidence intervals (CI) of the PK metrics comparted to previously reported values were calculated and assessed [4,5,20].

Table 1
LC-MS/MS parameters selected for the quantification of Molnupiravir active metabolite, NHC and Ribavirin (IS).

Analyte	Q1[a] (*m/z*)	Q3[b] (*m/z*)	DP[c] (V)	EP[d] (V)	CE[e] (V)	CXP[f] (V)
NHC	260.10	128.10	30.00	10.00	18.00	13.00
Ribavirin (IS)	245.10	113.20	40.00	10.00	15.00	15.00

[a] Q1, precursor ion.
[b] Q3, product ion.
[c] DP, declustering potential.
[d] EP, entrance potential.
[e] CE, collision energy.
[f] CXP, cell exit potential.

3. Results and discussion

3.1. Method development and optimization

The purpose of sample preparation is to reduce the effect of the biological and buffer matrix and to enhance the sensitivity and selectivity of the analysis. Liquid-liquid extraction (LLE) technique was applied using several organic solvents as well plasma protein precipitation using acetonitrile or methanol. As a result of the high polarity nature of NHC and for the simplicity and to minimize loss of samples, protein precipitation by acetonitrile followed by vacuum evaporation at 45 ℃ to enhance the sensitivity of the method was found to be the best method to demonstrate the maximum recovery in terms of inexpensiveness and easier plasma samples handling. Ribavirin was selected as IS as it has comparable physicochemical characteristics and extraction recovery as NHC, Fig. 1**C**.

Parameters of Mass Spectrometry were optimized to attain better selectivity without significantly compromising the sensitivity for the drug and IS, Table 1. Both + ESI and -ESI were investigated it was observed that the signals from + ESI were higher than those obtained from -ESI mode therefore + ESI mode was selected for NHC and IS using the following transitions: *m/z* 260.10 → 128.10 and 245.10 → 113.20, respectively, Fig. 2.

Different stationary phases were tried for chromatographic method optimization namely, Agilent Zorbax Eclipse plus C_{18}, 4.6 × 150 mm, (5 μm), Agilent Eclipse plus XDB-C_{18} column 4.6 × 100 mm, (3.5 μm), Agilent Eclipse plus C_{18}, 4.6 × 50 mm, (3.5 μm), Agilent Zorbax C_8 column 4.6 × 50 mm, (5 μm) and phenomenex kinetex C_8 column, 4.6 × 50 mm, (2.6 μm). Owing to the lower hydrophobicity of C_8 columns, its usage resulted in unsuccessful recovery of NHC peak from the endogenous matrix components. Trials using Agilent Eclipse plus C_{18}, 4.6 × 50 mm, (3.5 μm) displayed poor separation with unresolved peaks. Using Agilent Zorbax Eclipse plus C_{18}, 4.6 × 150 mm, (5 μm) gives the optimum performance in terms of proper separation and high resolution. Trials for mobile phase using methanol or acetonitrile with ammonium

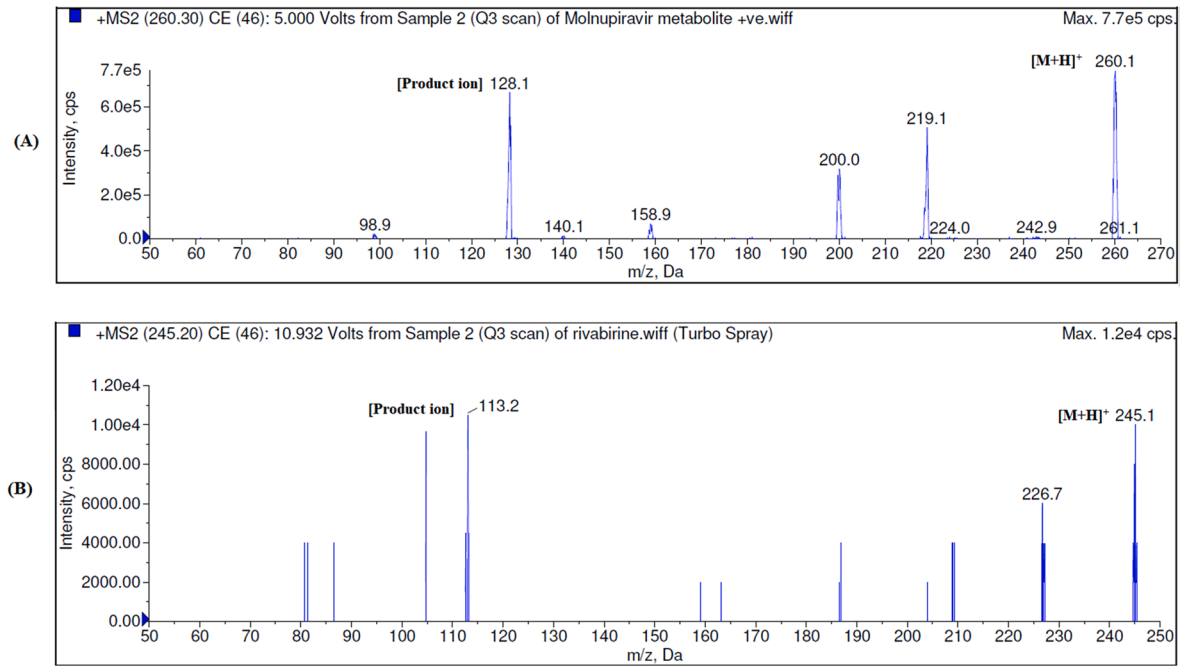

Fig. 2. Representative spectra for Molnupiravir active metabolite, NHC (A) and the internal standard, Ribavirin (B).

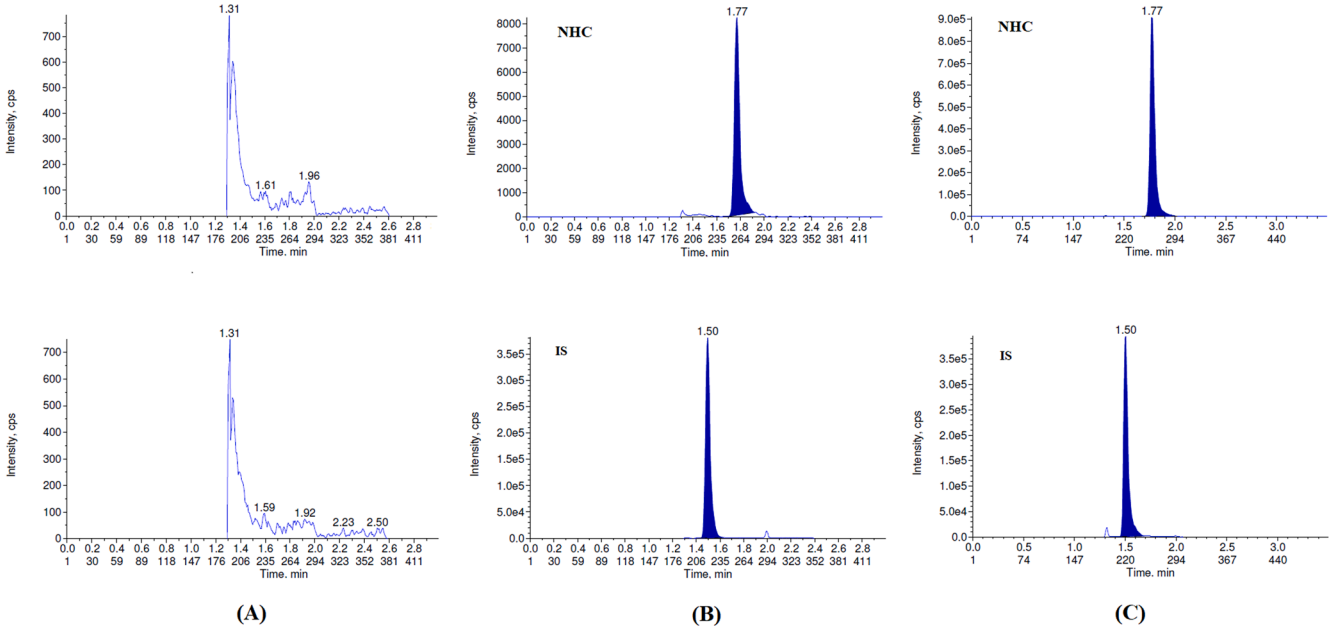

Fig. 3. Multiple reaction monitoring (MRM) chromatograms of: (A) blank plasma, (B) blank plasma spiked at LLOQ, (C) plasma samples of subject at 2 h after oral administration of one tablet containing MOL 800 mg.

formate and ammonium acetate buffer with varying combinations was tried also different proportions of 0.1% aqueous formic acid and 0.2% aqueous acetic acid was applied in an isocratic elution mode. Sharp and well-resolved peaks with minimum tailing were obtained using a combination of 0.2% acetic acid–methanol (95:5, *v/v*) at a flow rate of 0.3 mL/min. The retention times of NHC and IS were found to be 1.77 and 1.50 min, respectively, Fig. 3.

3.2. Method validation

3.2.1. Selectivity

Negligible interference was noticed from endogenous substances in each lot of blank plasma. Furthermore, no interference was shown at the retention times of the analyte and IS with the most commonly medications that co-administered in case of viral infections (ibuprofen, paracetamol, and diclofenac sodium) as shown in Fig. 3.

3.2.2. Calibration curve and quantitation range

Calibration curves were comprised of a blank, zero sample followed by calibration points. Six calibration curves were found to be linear covering the range of 20.0–10000.0 ng/mL for NHC by fitting the area ratio obtained against each concentration versus the amount of NHC. The r values, slopes and intercepts were calculated by applying weighted ($1/x^2$) method. The results of accuracy and precision for the lowest

Table 2
Intra- and Inter-day accuracy and precision results for Molnupiravir active metabolite, NHC.

Analyte	Concentration (ng mL^{-1})		Intra-day		Inter-day	
			RE (%)	RSD (%)	RE (%)	RSD (%)
NHC	LLOQ	20.0	−7.7	9.4	0.0	8.7
	Low QC	60.0	0.2	5.8	3.2	5.8
	Mid QC-A	800.0	4.0	0.9	5.1	3.3
	Mid QC-B	3000.0	2.4	2.9	1.0	4.3
	High QC	8000.0	−1.7	6.6	−0.9	5.1
n			6		18	

concentration (LLOQ) was satisfactory and fall within the acceptance limits, with RSD% less than 0.6% and accuracy vary from 99.0 to 105.2%.

3.2.3. Carry-over

Injection of blank samples after the upper limit of quantification sample (ULOQ, 10000.0 ng/mL) was used to evaluate the carry-over of the proposed method. the carry over in the blank samples didn't surpass 20% of LLOQ.

3.2.4. Accuracy and precision

The results of accuracy% for the intra-day accuracy were ranged from 92.34 to 103.95% and while for inter-day accuracy varied from 99.1 to 105.1%. The assay precision (Intra- and inter-day) was checked using 6 replicates of 4 concentrations for intra- and inter-day; correspondingly. The results of RSD% for the two types of precision was within the range of 0.7–9.4%, all results are summarized in Table 2.

3.2.5. Extraction recovery and matrix effect

The accuracy% results of NHC attained from 6 replicates of the three QC levels ranged from 78.2 to 80.1% whereas it was found to be 79.5% for IS. Matrix effect results were varied from 0.9 to 1.0 and 1.0 for IS. Furthermore, the IS-normalized matrix factor was found to have RSD% less than 4.0% the results were within the acceptance criteria and indicate that ion suppression or enhancement from the human plasma was consistent and don't interfere with the quantitation of analytes.

3.2.6. Dilution integrity

Spiked human plasma samples were diluted to obtain concentration of 8000.0 ng/mL aiming to test the dilution integrity of the method. Six determinations were diluted two and four folds with blank plasma samples were within method quantitation range. RSD% was found to be within 2.9 – 4.4% and accuracy results varied from 94.1 − 105.8%.

3.2.7. Stability

The stability of the spiked plasma samples under various temperature and timing conditions, in addition to the stability in stock standard solution was tested. NHC was found to be stable by standing for 18 h in human plasma at room temperature, and found to be stable by standing for 6 h in whole blood at room temperature. No significant loss was observed after storage of the processed plasma samples in the tray of the instrument's autosampler at 15 °C for 20 h. The long-term stability was tested for the low and high QC samples stored frozen at −70 ± 15 °C and found to be stable for 16 days. Spiked plasma samples were exposed to 5 FTC and found to be stable. The stability study results were within the acceptance criteria of ± 15% of the nominal concentration. Results were tabulated in Table 3. short-term storage of stock solution stability at 5 °C ± 3 °C was evaluated and found to be stable after 6 h and for long-term storage for 10 days for analyte. Stock solution stability for IS was found to be stable over 5 days.

3.2.8. Incurred plasma samples reanalysis

The percentage difference among the initial and repeated concentrations of the study samples was ranged from 1.8 to 15.3 %.

3.3. Data & population PK model of NHC, the active form of MOL

Table S2 describes the demographics and baseline laboratory values for the twelve healthy volunteers included in the PK model development process. All subjects were males, and all laboratory values were in the normal range. Fig. 4 shows the mean NHC plasma concentration–time curve.

The maximum plasma concentration (C_{max}) for NHC was 3640.43 ± 39.26 ng/mL and achieved at 1.5 h. Out of the total 132 measurable NHC concentrations, 15 observations (11.4 %) were below the quantification limit (BQLs). Four BQLs were observed at 0.25 h, two were observed at 9 h and nine were observed at 12 h post dose.

Fig. 5 shows schematic presentation of the final population PK model of NHC. The drug exhibits delayed absorption which was captured using a set of transit compartments where the drug transfers from one compartment to the subsequent one through first order transfer rate constant (K_{tr}). The average time the drug stays in the transit compartments is governed by mean transit time (M_{TT}). Following absorption to

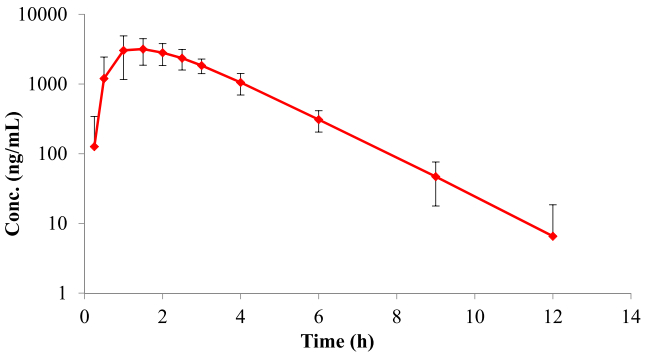

Fig. 4. Mean plasma concentration (±SD) following administration of single oral dose of Molnupiravir 800 mg tablets to 12 healthy volunteers (log-scale).

Table 3
Stability results for Molnupiravir active metabolite, NHC in human plasma at different conditions.

Analyte	Concentration (ng mL^{-1})		Short term stability at room temperature (18 h)			Freeze and thaw stability at −70°C (5 cycles)			Long term stability at −70°C (16 days)			Auto-sampler stability at 15°C (20 h)		
			Accuracy (%)	RSD (%)	Stability (%)	Accuracy (%)	RSD (%)	Stability (%)	Accuracy (%)	RSD (%)	Stability (%)	Accuracy (%)	RSD (%)	Stability (%)
NHC	Low QC	60.0	107.6	4.1	104.1	97.6	6.3	94.4	101.9	4.8	102.0	102.7	6.6	99.3
	High QC	8000.0	102.5	4.3	99.6	96.4	3.6	93.7	95.8	1.4	101.2	96.8	4.0	94.0
n			6			6			6			6		

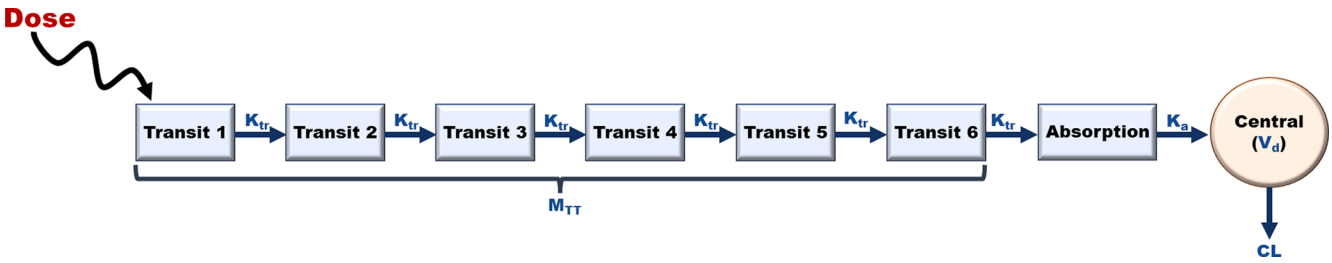

Fig. 5. A schematic presentation of MOL population pharmacokinetic model: following the tablet dose administration, the drug passes through a series of transit compartments till reaching the absorption compartment. The drug transfers from one transit compartment to the subsequent one through first order transfer rate constant (Ktr). The average time the drug stays in transit compartments (MTT) is equal to (n + 1)/Ktr, where n represents the number of transit compartments. Thereafter, the drug is absorbed to systemic circulation through first-order absorption rate constant (Ka). The drug follows one compartment disposition with apparent volume of distribution (Vd/F) and first-order apparent clearance (CL/F).

Table 4
Population PK parameter estimates and their associated Bootstrap estimates [a].

		Final Model Results		Bootstrap Results	
Population PK parameters	**Unit**	**Parameter Estimates**	**RSE (%)**	**Median values**	**95% CI**
K_{tr}	h^{-1}	14.4	29.2	15.4	7.9, 32.9
M_{TT}	h	0.5	12.3	0.5	0.4, 0.7
K_a	h^{-1}	2.3	24.4	2.1	1.3, 4.7
CL/F[b]	L/h·70 kg	75.2	4.3	83.5	71.3, 95.3
V_d/F[b]	L/70 kg	118.1	5.3	128.8	97.2, 154.9
BSV on K_{tr} [% shrinkage]	RSD%	65 [43.5]	37.2	57	19.0, 100.4
BSV on M_{TT} [% shrinkage]	RSD%	35 [9.19]	27	32	9.0, 53.2
BSV on K_a [% shrinkage]	RSD%	65 [34.7]	29.1	67	21.2, 124.4
BSV on CL/F [% shrinkage]	RSD%	14 [8.6]	25.3	22	7.8, 32.9
BSV on V_d/F [% shrinkage]	RSD%	15 [35.3]	33.3	19	3.7, 60.4
WT power exponent on CL/F		0.75*	NA		
WT power exponent on Vd/F		1*	NA		
Proportional error	%	19	8.7	19.5	15.8, 23.8

* Parameters fixed.
BSV: between-subject variability; CI: confidence interval; CL/F: apparent clearance; K_a: first order absorption rate constant from absorption compartment to central compartment; K_{tr}: first order transfer rate constant between transit compartments; M_{TT}: mean transit time; PK: pharmacokinetic; RSD: relative standard deviation; RSE: relative standard error; Vd/F: apparent volume of distribution; WT: body weight.
[a] Results are based on 500 bootstraps.
[b] Final covariate model: $CL/F = 75 \times (\frac{WT}{70})^{0.75}$; $V_d/F = 118 \times \frac{WT}{70}$

systemic circulation through first order absorption rate constant (K_a), a one compartment disposition model with linear elimination and proportional error best captured the NHC data.

Inclusion of body weight led to a significant improvement in the PK model (change in objective function from base model = − 13.4) with a reduction of 39 % and 25 % in IIV of CL/F and Vd/F, respectively. No other covariate was shown to be biologically and statistically correlated with PK parameters (Table S3 & Fig. S1). Equations (1) and (2) describe the final covariate models for CL/F and Vd/F, respectively:

$$CL \Big/ F_i = 75 \cdot \left(\frac{WT_i}{70}\right)^{0.75} \quad (1)$$

$$Vd \Big/ F_i = 118 \cdot \frac{WT_i}{70} \quad (2)$$

Table 4 shows the estimates and precision of final PK parameters. The typical value of CL/F for a subject with body weight of 70 kg was 75 L/h, the Vd/F was 118 L, the calculated half-life was 1.1 h, and the proportional error was 19%. The relative standard error estimates were lower than 30% and 35% for fixed and random effects, respectively indicating precision of PK parameters.

3.3.1. Population PK model evaluation

Fig. 6 shows the standard diagnostic plots for the developed population PK model. All plots demonstrate reasonable fitting and unbiased distribution of population predicted concentrations, individual predicted concentrations, and individual weighted residual. Fig. 7 shows representative individual fits for NHC concentration time profile. Table 4 demonstrates that the median PK parameter estimates, with their 95% CI obtained from 500 bootstraps are comparable to the estimates obtained from model fitting step proving the robustness of the estimation of the parameters. Fig. 8 shows the prediction corrected visual predictive check and indicates that the observed concentrations are in an agreement with model-based simulated concentrations.

3.3.2. Simulation to evaluate the current MOL dosing in egyptians

Simulations of current dosing regimen of 800 mg every 12 h for 5 days shows that the drug is completely eliminated before the administration of the subsequent dose, hence, no accumulation from previous doses occurs. Geometric means of simulation-based C_{max} and $AUC_{0\text{-}12}$ were 3827 ng/mL (GMR = 1.05; 90% CI = 0.96–1.15) and 9320 ng.h/mL (GMR = 1.04; 90% CI = 0.97–1.11), respectively.

Since the Egyptian population consists of a heterogenous population with genetic admixture, it is important to study the PK of MOL in this population to assess if any dose modifications are warranted [21]. Previous research did not reveal difference in PK between healthy and patients with COVID-19, hence, it is valid to extrapolate PK from healthy volunteers in our study and assume similar PK in Egyptian patients with COVID-19 [21,22]. Our analysis showed that the estimated CL/F, Vd/F and half-life for NHC were 75 L/h·70 kg, 118 L/70 kg, and 1.1 h, respectively. These parameter estimates were comparable to previous analysis where the estimated values for the same parameters were 76.9 L/70 kg, 142 L/70 kg, and 1.29 h, respectively [4].

Our results demonstrated that body weight was a significant covariate that explained IIV of both CL/F and Vd/F. This finding matches a previous analysis showing the importance of body weight as a covariate to be associated with both PK parameters and insignificance of other covariates specifically liver and renal functions given the elimination

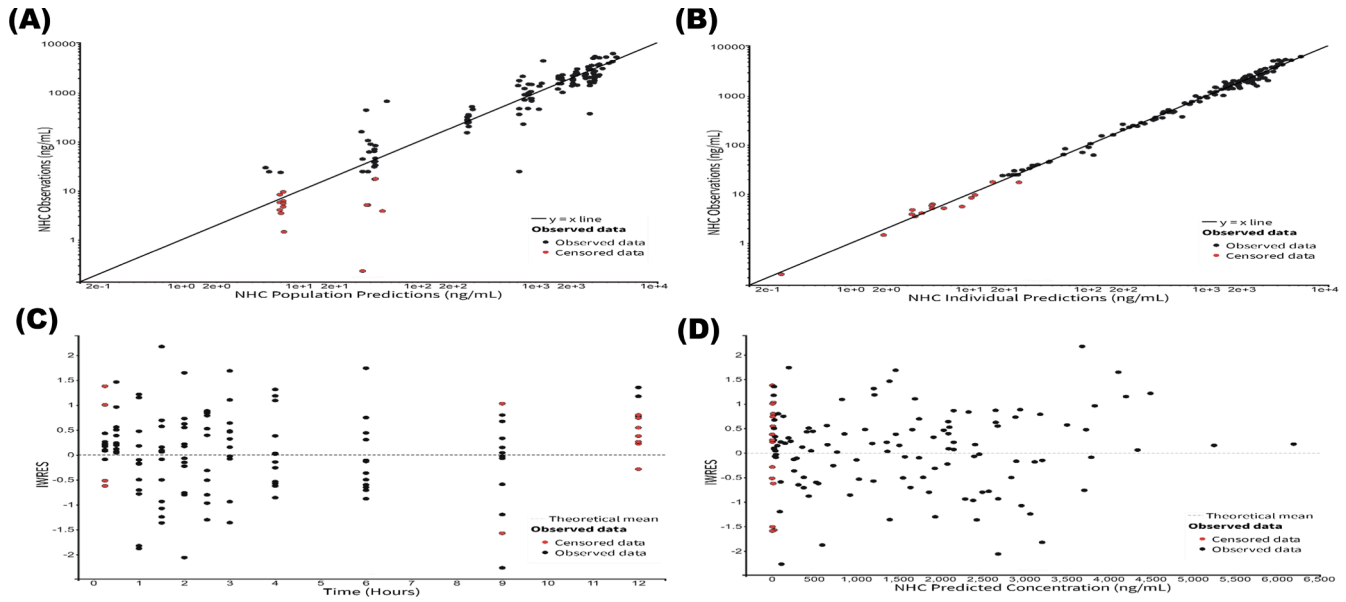

Fig. 6. Diagnostic plots of population pharmacokinetic model of NHC depicted by transit compartments for absorption process and one compartment disposition with linear elimination from systemic circulation and proportional error model: (A) observations versus population predictions for NHC (ng/mL), (B) observations versus individual predictions for NHC, (C) Individual weighted residuals (IWRES) vs time after the dose for NHC, (D) IWRES vs population predictions for NHC. Black line in (A, B) represents the line of unity while the dotted black horizontal line in (C, D) represents the theoretical mean value of zero for IWRES. Concentrations above the lower limit of quantification (LLOQ = 20 ng/mL) are colored in black while censored concentrations are colored in red.

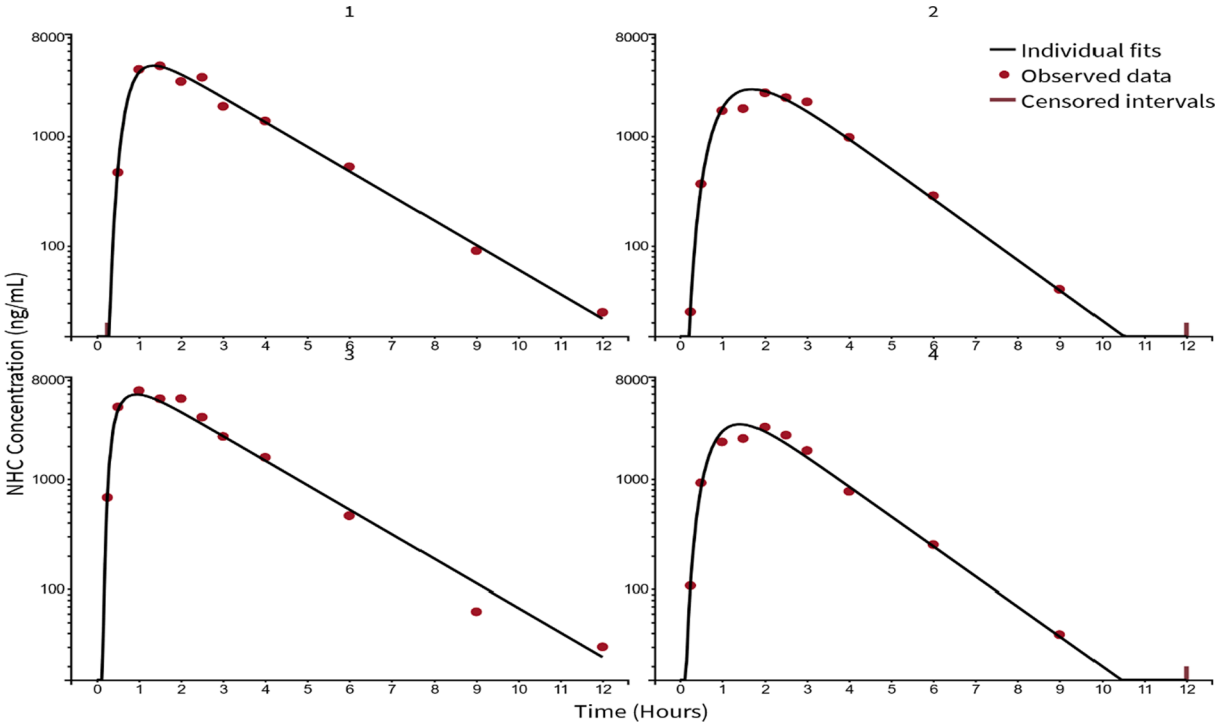

Fig. 7. Representative Individual fits of population pharmacokinetic model of NHC depicted by transit compartments for absorption process and one compartment disposition with linear elimination from systemic circulation and proportional error model: Black lines represent the predicted NHC concentrations (ng/mL) and red circles indicates the observed NHC concentrations (ng/mL). Brown rectangular shaded areas represents censored intervals for observations below the quantification limit (20 ng/mL).

mechanism of the drug through esterases and kinases [4]. However, previous analysis showed that females had 31.3% decrease in Vd/F compared to males which was associated with 11% increase in $AUC_{0\text{-}12}$. However, studying sex effect on Vd/F and $AUC_{0\text{-}12}$ was not feasible since all subjects in our study were males.

Our simulations showed that the median C_{max}, the PK metric for safety, and $AUC_{0\text{-}12}$, the PK metric for efficacy, were 3827 ng/mL and 9320 ng.h/mL, respectively. The simulations are comparable to previous analysis where the reported values for both PK metrics were 3640 ng/mL and 8720 ng.h/mL following the administration of 800 mg of MOL [22]. Consequently, the current dosing recommendations of MOL are sufficient to ensure efficacy and safety in the Egyptian population.

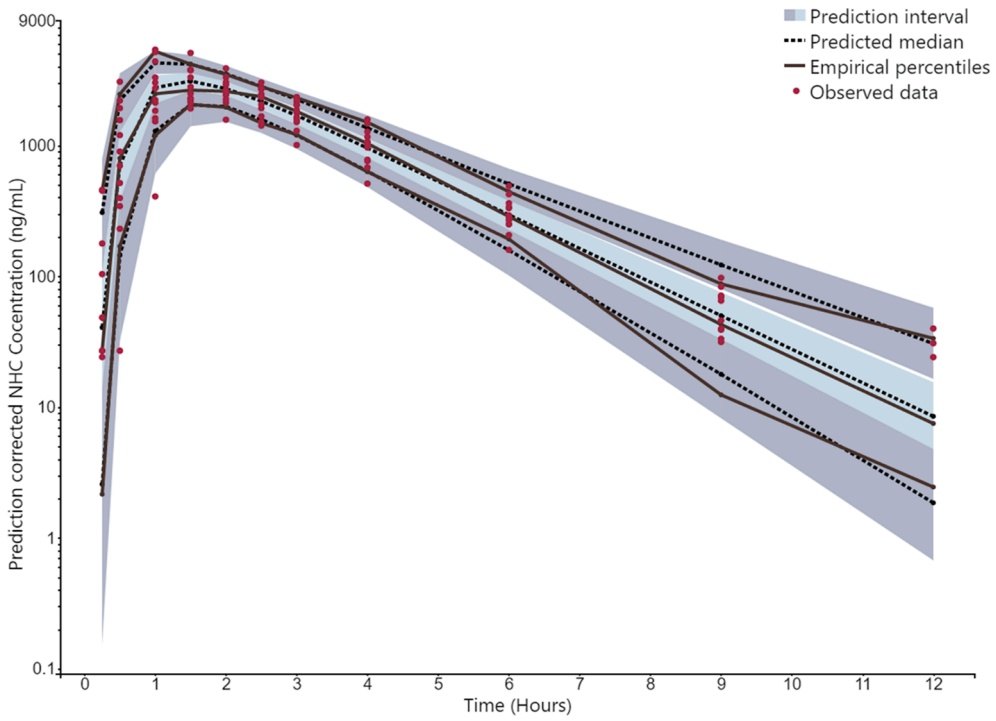

Fig. 8. Prediction-Corrected Visual predictive check for the population pharmacokinetic model: red circles represent the observations, the brown solid lines represent the 5th, 50th and 95th empirical percentiles, the black dashed lines represent the median 5th, 50th and 95th percentiles of the predictions with the shaded area around the lines representing the 90% confidence interval (n = 500).

4. Conclusion

A reliable and selective LC-MS/MS bioanalytical method has been developed and fully validated to determine of NHC in human plasma. The results of the proposed method were satisfactory and proved the selectivity, accuracy and precision over the concentration range that allowed the estimation of plasma concentrations of the studied drug effectively. In addition, population PK model was developed for NHC. Simulations showed that current MOL dosage can achieve the therapeutic targets and dose adjustment may not be required for the Egyptian population. The developed model could be used in the future to refine MOL's dosage once further therapeutic targets are established.

Declaration of Competing Interest

The authors declare that they have no known competing financial interests or personal relationships that could have appeared to influence the work reported in this paper.

Acknowledgement

Authors gratefully acknowledge the support received from Zi Diligence biocenter for their sincere and efficient contribution in completing this research work. Also, wish to thank Eva pharma, Egypt, for sponsoring this research work and supplying the resources (e.g. test and standard materials).

Appendix A. Supplementary material

Supplementary data to this article can be found online at https://doi.org/10.1016/j.jchromb.2022.123363.

References

[1] M. Imran, M. Kumar Arora, S.M.B. Asdaq, S.A. Khan, S.I. Alaqel, M.K. Alshammari, M.M. Alshehri, A.S. Alshrari, A. Mateq Ali, A.M. Al-Shammeri, B.D. Alhazmi, A.A. Harshan, M.T. Alam, Abida, Discovery, Development, and Patent Trends on Molnupiravir: A Prospective Oral Treatment for COVID-19, Molecules 26 (2021).

[2] M.I. Morsy, E.G. Nouman, Y.M. Abdallah, M.A. Zainelabdeen, M.M. Darwish, A. Y. Hassan, A.S. Gouda, M.R. Rezk, A.M. Abdel-Megied, H.M. Marzouk, A novel LC-MS/MS method for determination of the potential antiviral candidate favipiravir for the emergency treatment of SARS-CoV-2 virus in human plasma: Application to a bioequivalence study in Egyptian human volunteers, J. Pharm. Biomed. Anal. 199 (2021), 114057.

[3] M.R. Rezk, K.A. Badr, N.S. Abdel-Naby, M.M. Ayyad, A novel, rapid and simple UPLC-MS/MS method for quantification of favipiravir in human plasma: Application to a bioequivalence study, Biomedical chromatography : BMC 35 (2021), e5098.

[4] EMA Assessment report, Use of molnupiravir for the treatment of COVID-19, EMA/719664/2021 Corr. 1, Committee for Medicinal Products for Human Use (CHMP), 2021.

[5] W.P. Painter, W. Holman, J.A. Bush, F. Almazedi, H. Malik, N. Eraut, M.J. Morin, L. J. Szewczyk, G.R. Painter, Human Safety, Tolerability, and Pharmacokinetics of Molnupiravir, a Novel Broad-Spectrum Oral Antiviral Agent with Activity Against SARS-CoV-2, Antimicrob. Agents Chemother. (2021).

[6] ELSevier, https://elsevier.health/en-US/preview/molnupiravir#pharmacokinetics., 2022.

[7] Merck and Ridgeback's Investigational Oral Antiviral Molnupiravir Reduced the Risk of Hospitalization or Death by Approximately 50 Percent Compared to Placebo for Patients with Mild or Moderate COVID-19 in Positive Interim Analysis of Phase 3 Study, Merck, 2021.

[8] T.L. Parsons, L.A. Kryszak, M.A. Marzinke, Development and validation of assays for the quantification of beta-D-N(4)-hydroxycytidine in human plasma and beta-D-N(4)-hydroxycytidine-triphosphate in peripheral blood mononuclear cell lysates, Journal of chromatography, B, Analytical technologies in the biomedical and life sciences 1182 (2021), 122921.

[9] A. Amara, S.D. Penchala, L. Else, C. Hale, R. FitzGerald, L. Walker, R. Lyons, T. Fletcher, S. Khoo, The development and validation of a novel LC-MS/MS method for the simultaneous quantification of Molnupiravir and its metabolite ss-d-N4-hydroxycytidine in human plasma and saliva, J. Pharm. Biomed. Anal. 206 (2021), 114356.

[10] FDA, Guidance for Industry (2018). Bioanalytical method validation. US department of health and human services, center for drug evaluation and research and center for veterinary medicine, US Food and Drug Administration, 2018.

[11] M.R. Rezk, E.B. Basalious, K.A. Badr, Novel determination of sofosbuvir and velpatasvir in human plasma by UPLC-MS/MS method: Application to a bioequivalence study, Biomedical chromatography : BMC 32 (2018), e4347.

[12] M.R. Rezk, K.A. Badr, Quantification of amlodipine and atorvastatin in human plasma by UPLC-MS/MS method and its application to a bioequivalence study, Biomedical chromatography : BMC 32 (2018), e4224.

[13] M.R. Rezk, K.A. Badr, Determination of amlodipine, indapamide and perindopril in human plasma by a novel LC-MS/MS method: Application to a bioequivalence study, Biomedical chromatography : BMC 35 (2021), e5048.
[14] H.M. Marzouk, M.R. Rezk, A.S. Gouda, A.M. Abdel-Megied, A novel stability-indicating HPLC-DAD method for determination of favipiravir, a potential antiviral drug for COVID-19 treatment; application to degradation kinetic studies and in-vitro dissolution profiling, Microchemical journal : devoted to the application of microtechniques in all branches of science 172 (2022), 106917.
[15] M.R. Rezk, K.A. Badr, Development, optimization and validation of a highly sensitive UPLC-ESI-MS/MS method for simultaneous quantification of amlodipine, benazeprile and benazeprilat in human plasma: application to a bioequivalence study, J. Pharm. Biomed. Anal. 98 (2014) 1–8.
[16] D.R. Mould, R.N. Upton, Basic concepts in population modeling, simulation, and model-based drug development-part 2: introduction to pharmacokinetic modeling methods, CPT: pharmacometrics & systems pharmacology 2 (2013), e38.
[17] P. Traynard, G. Ayral, M. Twarogowska, J. Chauvin, Efficient pharmacokinetic modeling workflow with the MonolixSuite: a case study of remifentanil, CPT Pharmacometrics Syst. Pharmacol. 9 (4) (2020) 198–210.
[18] S.L. Beal, Ways to fit a PK model with some data below the quantification limit, J. Pharmacokinet Pharmacodyn. 28 (2001) 481–504.
[19] G.B. West, J.H. Brown, B.J. Enquist, A general model for the origin of allometric scaling laws in biology, Science 276 (1997) 122–126.
[20] A. Jayk Bernal, M.M. Gomes da Silva, D.B. Musungaie, E. Kovalchuk, A. Gonzalez, V. Delos Reyes, A. Martín-Quirós, Y. Caraco, A. Williams-Diaz, M.L. Brown, J. Du, A. Pedley, C. Assaid, J. Strizki, J.A. Grobler, H.H. Shamsuddin, R. Tipping, H. Wan, A. Paschke, J.R. Butterton, M.G. Johnson, C. De Anda, Molnupiravir for Oral Treatment of Covid-19 in Nonhospitalized Patients, N. Engl. J. Med. 386 (6) (2022) 509–520.
[21] J.R. Luis, D.J. Rowold, M. Regueiro, B. Caeiro, C. Cinnioğlu, C. Roseman, P. A. Underhill, L.L. Cavalli-Sforza, R.J. Herrera, The Levant versus the Horn of Africa: evidence for bidirectional corridors of human migrations, Am. J. Hum. Genet. 74 (3) (2004) 532–544.
[22] Antimicrobial Drugs Advisory Committee Meeting Announcement - 11/30/2021 - 11/30/2021. FDA, in: ttps://www.fda.gov/advisory-committees/advisory-committee-calendar/november-30-2021-antimicrobial-drugs-advisory-committee-meeting-announcement-11302021-11302021 (Ed.), November 30, 2021.